JOURNAL OF MATERIALS SCIENCE 29 (1994) 6221 - 6226

The microstructure and interface behaviour of Ni/NiAl composites produced by the explosive compaction of powders

J. BYSTRZYCKI, J. PASZULA, R. TREBINSKI
Department of Metallurgy and Metal Technology, Faculty of Chemistry and Technical Physics, Military University of Technology, 00-908 Warsaw, Poland

R. A. VARIN
Department of Mechanical Engineering, University of Waterloo, Waterloo, Ontario, Canada, N2L 3G1

Explosive compaction of Ni and NiAl powders was utilized for the processing of Ni/NiAl metal-matrix composites containing up to 57 vol % NiAl particulate. The microstructure, the Vickers microhardness and the Ni/NiAl interfacial bonding strength were studied. The resulting microstructure had a very low volume fraction of porosity (~ 1 vol %) except for the melting zone formed in the upper portion of a cylindrical specimen. NiAl particles underwent welding during explosive compaction; this was particularly pronounced at the highest volume fractions of NiAl. The lowest microhardness of the Ni matrix was observed in the central portion of a cylindrical specimen. Other parts of the matrix were heavily cold-worked, indicating that a recrystallization had occurred in the centre. NiAl particles were also highly cold-worked regardless of their volume fraction in the composite. The Ni/NiAl interfacial bond strength, measured by the indentation debonding technique, was highest in a composite containing 57 vol % of NiAl particulate.

1. Introduction

Although the B2 cubic-crystal-structure intermetallic NiAl has many attractive features (such as a relatively high melting point, a density reduced by one third compared to Ni-base superalloys and excellent oxidation resistance), its use as a high-temperature structural alloy is limited by its low room-temperature toughness (brittleness) and inadequate creep properties.

One potential route for improving the toughness is to utilize a fibrous second phase for reinforcement. Ceramic particulates can also be used for strength improvements. Some efforts were made in the past to fabricate both ceramic particulate composites and aligned chopped fibrous composites with a NiAl matrix using powder metallurgy (P/M) techniques, such as reactive sintering and powder injection moulding [1]. P/M techniques utilizing both cold and hot isostatic pressing (CIP and HIP, respectively) were also used to fabricate Nb and Ti alloyed NiAl with a resulting almost fivefold increase in the fracture toughness [2].

However, all conventional P/M techniques involve quite sophisticated equipment (for example, for HIPing) and elaborate, and usually quite long, pressing cycles at very high temperatures to achieve a fully dense monolithic NiAl or its composite. A much faster method of powder consolidation would be an explosive compaction which, to the best of our knowledge, has never been utilized for the fabrication of an intermetallic composite. The only studies, known to us, devoted to fabricating NiAl and Ni_3Al intermetallics from elemental powders, were reported by Arkens *et al.* [3], Horie *et al.* [4, 5] and Song *et al.* [6]. However, explosively compacted specimens have also been additionally HIPed to remove an excessive porosity [3].

This paper summarizes efforts to fabricate an NiAl-bearing particulate composite by the explosive compaction of powders. An Ni powder was mixed with an NiAl powder to provide a ductile matrix (binder) in the fabricated composite. Composites containing 8, 30 and 57 vol % of the NiAl particulate were fabricated. Their microstructure and microhardness and the Ni/NiAl interfacial properties, reflecting the quality of the bonding, are described and discussed.

2. Experimental procedure

The explosive-compaction treatment was used to produce three different Ni–NiAl composites. The characteristic of the Ni and NiAl powders used in this study are summarized in Table I. Elemental powders were mixed to yield target compositions corresponding to 5, 25 and 50 vol % of NiAl.

The experimental set-up for the compaction of the intermetallic powders consisted of a cylindrical container (with an inner diameter of 8 mm and an outer

0022–2461

TABLE I Material characteristics

Powder	Size (μm)	Shape	Process
Ni	5–8	Spherical	Carbonyl
NiAl	16–20	Angular	Milled

TABLE II Important parameters of the explosives

Explosive	Detonation velocity ($m s^{-1}$)	Density ($kg m^{-3}$)	Pressure (GPa)
AMN3	3000	920	2.5
MWZHx20	5600	1460	12

diameter of 18 mm) filled with compacted powder and closed by a steel plug, a momentum trap, a cylindrical charge of explosive surrounding the container (outer diameter 64 mm), and a plane-wave generator and primer. A two-stage compaction procedure was performed. In the first shot, the initial densification of the compacted powder was performed by the use of an AMN3 explosive. The final consolidation was achieved in the second shot by the use of a MWZHx20 explosive. Table II shows some important parameters of the explosives used.

After the explosive treatment, all the materials were turned on a lathe to yield cylindrical samples about 6 mm in diameter. Metallographic specimens were cut from the as-received materials, mounted in Bakelite and wet-ground on 100, 200, 400 and 600 grit silicon-carbide (SiC) paper, using water as a lubricant and then they were mechanically polished with 1.0, 0.3 and 0.05 μm alumina based powder. The grain morphology of the Ni-matrix was revealed using an etch comprising of a mixture of HNO_3, CH_3COOH and H_2O in the proportions 65:18:17, respectively. The microstructure of all the composites was examined (in both the longitudinal and the transverse cross-sections) by optical microscopy.

The density was measured for all the composite specimens by the Archimedean method. The porosity, NiAl particle size and the real volume fraction of NiAl were all measured using a Java image-analysis package (from Jandel) [7].

Vickers-microhardness testing with a 25 g load was performed to analyse the microhardness distribution along the diameter on the transverse cross-section of the cylindrical composite specimens. Vickers indentation with a 100 g load was used to induce the Ni/NiAl-interface debonding [8] whose length was measured using the Java image-analysis system.

The Ni/NiAl interface characteristics were observed by optical and scanning electron microscopy (SEM). Fully quantitative X-ray energy dispersive spectroscopy (EDS, with a QX 2000 Link System with high-purity elemental standards) was used to determine the chemical composition across the Ni/NiAl interface; an electron probe with a 0.01 μm diameter was used.

3. Results and discussion

3.1. Microstructure and microhardness

Typical photomicrographs of the transverse cross-sections of the Ni/NiAl composites with various volume fractions of the NiAl particulate are given in Fig. 1. Slight increases in the porosity and larger NiAl particulate sizes can be seen as the volume fraction of the NiAl increases. Details of the microstructural characterization of composites are given in Table III. The measured volume fractions of the NiAl particulate are slightly higher than the target values (5, 25 and 50 vol % NiAl). An increase in the size of NiAl

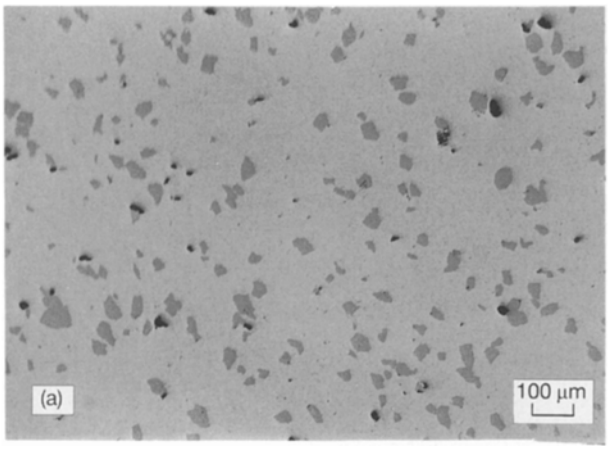

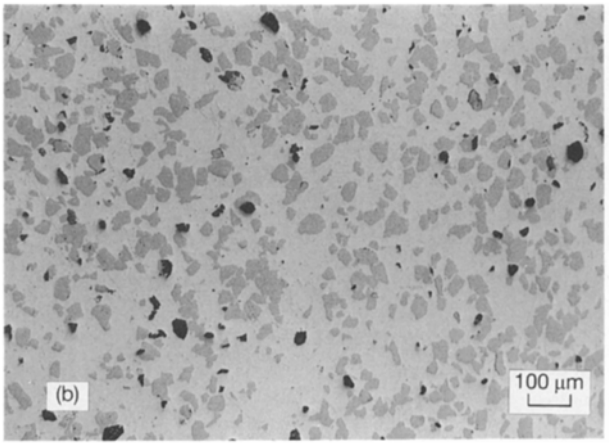

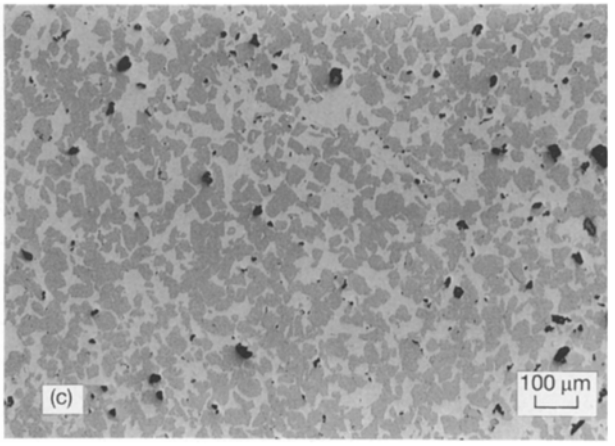

Figure 1 Photographs of the microstructure (transverse cross-section) of the explosively compacted Ni/NiAl composite: (a) 8.5 vol % NiAl, (b) 30.3 vol % NiAl, and (c) 56.6 vol % NiAl.

TABLE III Volume fractions of the porosity and of the particles of NiAl in the Ni–NiAl composites and the density of the composites after explosive compaction

Fraction of NiAl (vol %)	Porosity (%)	NiAl particle size (μm)	Ni-matrix grain size (μm)	Density of the composite ($kg\,m^{-3}$)
8.5 ± 0.7	1.5 ± 0.4	23.96 ± 8.03	5.8 ± 1.7	8262.22
30.3 ± 2.2	1.6 ± 0.3	25.36 ± 9.96	7.0 ± 1.2	7578.87
56.6 ± 4.8	1.7 ± 0.3	35.75 ± 18.40	8.0 ± 2.2	6752.56

may result from a welding of the individual NiAl particles during explosive compaction; this seems to occur more intensely as the volume fraction of NiAl increases. For example, the average size of the NiAl particles for 56.6 vol% NiAl is around 36 μm (Table III), which is twice as large as the initial size of the NiAl powder (16 μm, Table I). On the other hand, the average grain size of the Ni matrix (binder) in the compacted composite (about 6 μm, Table III) is not very different than the initial size of the Ni powder (5–8 μm, Table I). Although the porosity slightly increases as the volume fraction of NiAl increases, it is still very low and does not exceed 1.7% (Table III). For the sake of clarity, it must be stated that the upper part of a compacted cylindrical specimen contained a centrally located melted zone (which formed as a result of the high-explosive energy) which exhibited a much higher porosity. However, by a careful adjustment of the detonation parameters, the formation of this melted zone could be prevented.

To assess more closely the changes in the NiAl-particle morphology a Ferret coefficient, α, expressed as a planar ratio of a vertical-to-horizontal diameter of a particle [9], was calculated for all three composites and the results are given in Fig. 2 as a function of the volume fraction of NiAl. Note that $\alpha = 1$ represents an ideal circular (spherical) particle and it can be seen that up to about 30 vol % NiAl all the NiAl particles are characterized by $\alpha \approx 1$. However, at 57 vol %, the NiAl particles are characterized by $\alpha \approx 2$, which indicates particles elongated along the longitudinal axis of a cylindrical composite specimen.

The density of a Ni/NiAl composite decreases as the volume fraction of NiAl increases, approaching $6800\,kg\,m^{-3}$ at 57 vol % NiAl (Table III). A comparison of the composite density with densities of both Ni [10] and NiAl [11] is presented in Fig. 3. A substantial drop in the density of the composite (compared to Ni) can clearly be seen. This is obviously very advantageous for any potential structural application.

The Vickers microhardness (VHN), with a 25 g load, of the Ni matrix was measured along the diameter of the compacted cylindrical composite specimens and the results are plotted in Fig. 4. It can be observed that the minimum of the microhardness occurs at the centre of the composite specimen, whatever the volume fraction of the NiAl particulate is. Such a distribution of the microhardness indicates that the Ni matrix which is further away from the centre is cold worked and that the matrix close to the centre undergoes recrystallization. This is possible because the distribution of the detonation energy during explosive compaction exhibits a peak around the centre of cylindrical, compacted specimens, leading to a certain (not measured) increase in temperature. The fact that an increase in temperature did indeed occur during compaction is, as has already been mentioned, confirmed by the observation of a

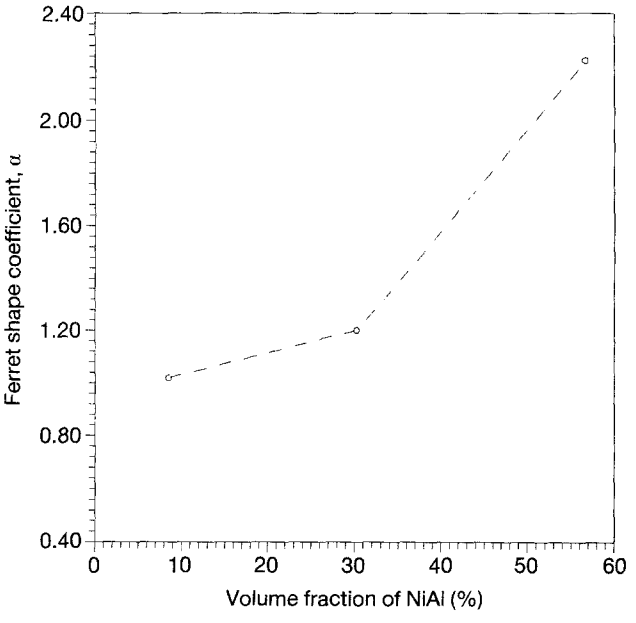

Figure 2 The Ferret shape coefficient, α, of the NiAl particles as a function of the volume fraction of the NiAl particles.

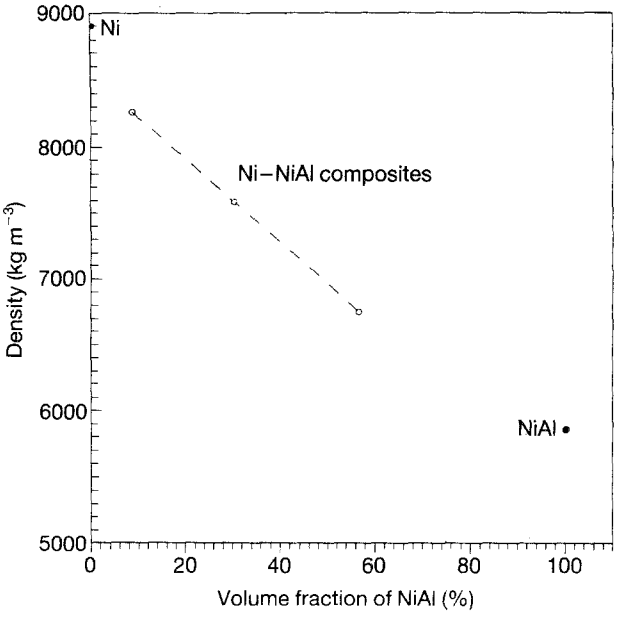

Figure 3 The density of the explosively compacted Ni/NiAl composite as a function of the NiAl content. (Values for Ni [10] and NiAl [11] are given for comparison.)

TABLE IV The Al concentration near the interface measured by EDS in the Ni–NiAl composites

Fraction of NiAl (vol %)	Al concentration (at %) at various distance from the interface				
	NiAl		Interface	Ni	
	2 μm	1 μm	0 μm	1 μm	2 μm
8.5	46.2 ± 0.2	42.7 ± 0.5	32.6 ± 5.8	4.2 ± 1.8	0.7 ± 0.3
30.3	46.2 ± 0.3	42.5 ± 0.3	33.8 ± 5.6	5.0 ± 2.2	0.6 ± 0.1
56.6	46.2 ± 0.3	43.2 ± 0.9	26.3 ± 2.4	4.5 ± 2.4	0.5 ± 0.2

An average of five readings were taken for each data point in the table, the standard deviations are shown by the plus-or-minus values.

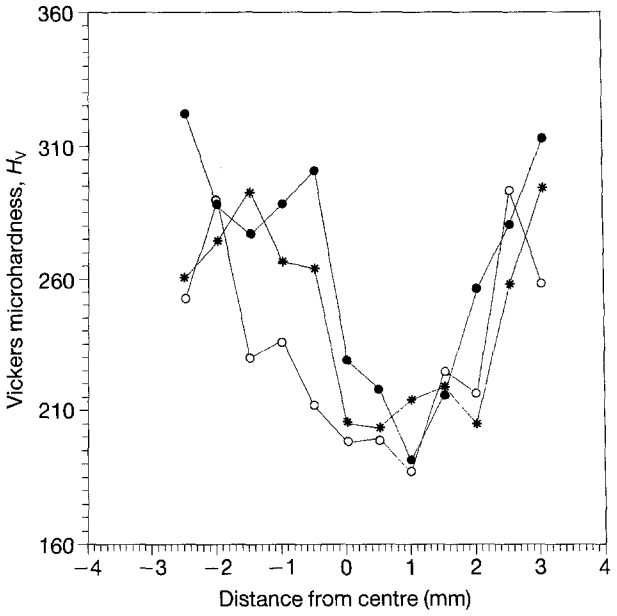

Figure 4 The Vickers microhardness H_v for a 25 g load, of the Ni matrix measured along the diameter of the explosively compacted Ni/NiAl specimens: (○) 56.6 vol % NiAl, (∗) 30.3 vol % NiAl, and (●) 8.5 vol % NiAl.

melted zone in the upper portion of the cylindrical compacted specimens.

Also, the value of H_v, for a 25 g load, for the NiAl particles in the composite was measured, and the mean values with the standard deviations (for ten indentations) are 512 ± 25, 507 ± 32 and 491 ± 10 kg mm^{-2} for 8.5, 30.3 and 56.6 vol % of NiAl, respectively. Apparently, H_v does not depend on the volume fraction of the particles despite some welding of the powder particles occurring (particularly at higher volume fractions of NiAl, Table III). Obviously, the Vickers microhardness of NiAl (for a load of 25 g) is much higher than that of the Ni matrix, indicating the high reinforcing potential of the NiAl particles. However, the value of H_v for intermetallics (and for many other metallic materials) often increases as the indentation loads decrease [12]; this is most probably because of friction between the microhardness indenter and the test specimen [13, 14]. However, the H_v values of NiAl particles in the composite seem to be unusually high to be exclusively due to the effect of decreasing indentation loads. To solve this dilemma, the Vickers microhardness at 25 g was measured for two batches of hot extruded, monolithic NiAl with the following compositions: 53.4(± 0.2)at%Ni–46.6 (± 0.2)at % Al and 53.3 ± (0.5)at % Ni–46.7(± 0.5) at % Al (for an average of five EDS readings). These compositions are almost exactly the same as the composition of the NiAl particles in the explosively compacted composites, that is 53.3(± 0.5)at % Ni–46.7(± 0.5)at % Al. The H_v values obtained for a monolithic NiAl were 356 ± 30 and 395 ± 11 kg mm^{-2} (for an average of ten indentations). It is quite clear that the NiAl particulate in the composite is much harder (for a 25 g indentation load) than monolithic NiAl. Apparently, the NiAl particles are heavily cold worked as a result of explosive compaction.

3.2. Interface characterization

It was observed that indenting the composite under higher loads (of order 1000–2000 g) resulted in the debonding cracking, on many occasions, of the interfaces of the NiAl particles surrounding the indentation (Fig. 5).

In order to investigate the strength of the bonding between the Ni matrix and the NiAl particles, an indentation debonding method, recently developed in our laboratory [8], was used. In this method, a Vickers indenter is pushed close to the vicinity of an interface and the total debonding length (an interface crack) is measured. An example is shown in Fig. 6. Although the above method is qualitative in its nature, it is useful for comparative purposes.

Fig. 7 shows the calculated mean value of the debonding length for ten particle (the standard deviations are shown by the bars) as a function of the

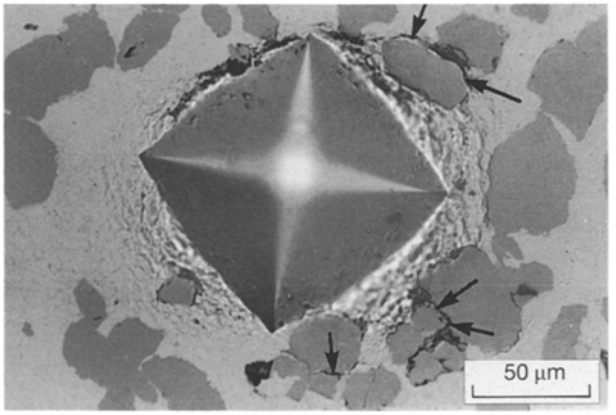

Figure 5 A photomicrograph of the debonding (shown by the arrows) at the NiAl particle interfaces which is induced by an indentation load of 2000 g in the 56.6 vol % NiAl composite.

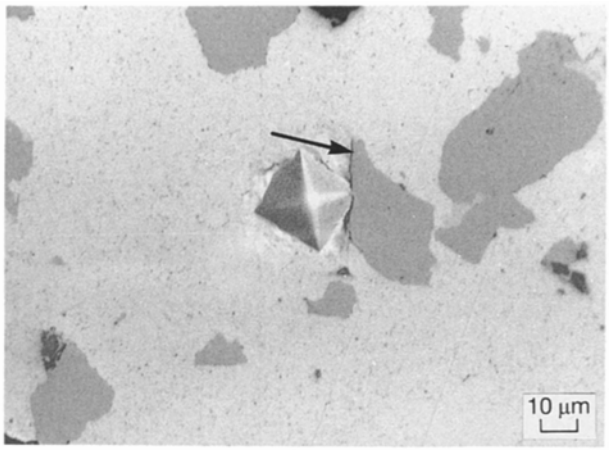

Figure 6 A photomicrograph of the indentation debonding for a 100 g load in the 30.3 vol % NiAl composite. The debonding length is indicated by the arrow.

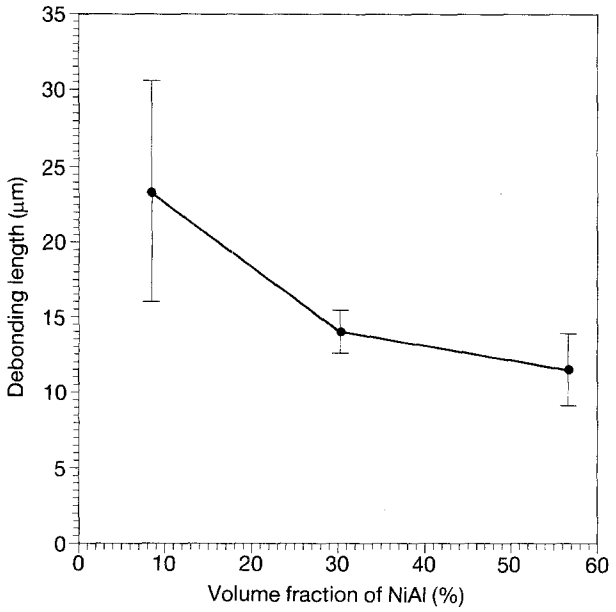

Figure 7 The debonding length for a 100 g load at the Ni/NiAl interface as a function of the volume fraction of the NiAl particulate.

volume fraction of the NiAl particulate. It can be observed that the shortest debonding length, and hence the highest interfacial bond strength between the Ni matrix and the NiAl particles, occurs in the composite with the highest volume fraction of NiAl reinforcement. In order to investigate the possible cause of this behaviour, EDS measurements of the Al distribution across the Ni/NiAl interface were carried out using the smallest available probe size of 0.01 μm. The results with standard deviation bars (for five readings) are presented in Fig. 8. It can be observed that the interfacial diffusion zone is very narrow and that it does not exceed 1 μm. Therefore, the bonding character seems to be more mechanical rather than diffusional. More importantly, the concentration of Al and the resulting diffusion zone thickness are the same (within the experimental accuracy) for all three composites with various volume fractions of the NiAl particulates. Therefore, the reason why the Ni/NiAl interfacial bond is strongest in the composite with the highest volume fraction of NiAl remains unclear.

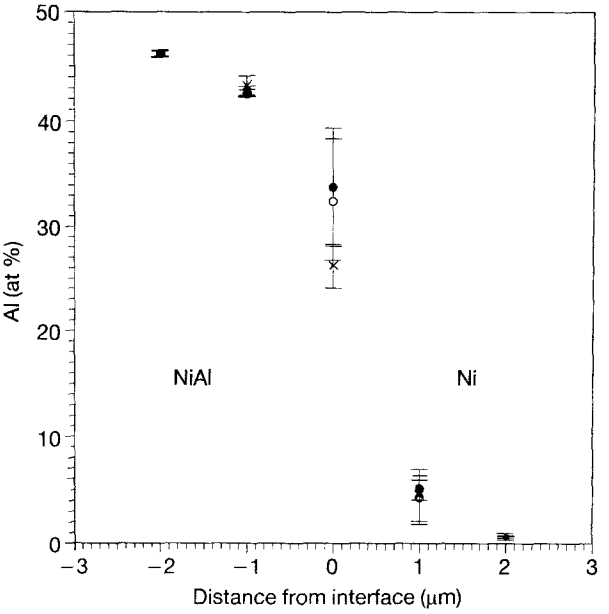

Figure 8 EDS measurements of the Al concentration across the Ni/NiAl interface in three composites: (○) 8.5 vol % NiAl, (●) 30.3 vol % NiAl, and (✳) 56.6 vol % NiAl.

4. Conclusions

Ni-matrix composites containing up to about 60 vol % of NiAl particulate can be fabricated by the explosive compaction of Ni and NiAl powders. The resulting microstructure has a very low volume fraction of porosity with a maximum of 1% except for the melting zone which appears in the upper portion of cylindrical specimens. This zone can be eliminated by adjustment of the detonation parameters. The grain size of the Ni matrix after compaction remains essentially the same as the initial size of the Ni powder. The NiAl particles undergo welding, particularly at the highest volume fraction of NiAl. The lowest microhardness of the Ni matrix, measured across the diameter, is observed in the central portion of the cylindrical specimens. This is most probably a result of recrystallization occurring because of a distribution of the energy of the shock compression (with the maximum at the centre of the specimen). The Ni matrix further from the centre exhibits a very high Vickers microhardness, indicating heavy cold working. The NiAl particles in the composite are also heavily cold worked, as indicated by their unusually high Vickers microhardness. The Ni/NiAl interfacial bond strength is highest in the composite with the highest volume fraction of NiAl. The cause of this behaviour is unclear.

Acknowledgements

This research was performed during Dr J. Bystrzycki's scientific internship at the Department of Mechanical Engineering of the University of Waterloo. The Financial support of grants from the Polish Committee for Scientific Research (research project number 709549101) and the Natural Sciences and Engineering Research Council of Canada is gratefully acknowledged.

References

1. D. E. ALMAN and N. S. STOLOFF, *Int. J. Powder Metall.* **27** (1991) 29.
2. W. A. KAYSSER, R. LAAG, J. C. MURRAY and G. E. PETZOW, *ibid.* **27** (1991) 43.
3. O. ARKENS, L. DELAEY, J. DE TAVERNIER, B, HUYBRECHTS, L. BUEKENHOUT and J. C. LIBOUTON, in "High Temperature Ordered Intermetallic Alloys III", edited by L. C. Liu, A. I. Taub, N. S. Stoloff and C. C. Koch, Vol. 133 (Materials Research Society, Pittsburgh, PA, 1989) pp. 493–498.
4. Y. HORIE, R. A. GRAHAM and I. K. SIMONSEN, in "Metallurgical Applications of Shock-wave and High Strain Rate Phenomena", edited by L. E. Murr, K. P. Staudhammer, M. A. Meyers (Marcel Dekker, New York, 1986).
5. *Idem., Mater. Lett.* **3** (1985) 354.
6. I. SONG, N. N. THADDANI and J. DING, in Proceedings of the 10th High Energy Rate Forming Conference, Ljublana, 1989, p. 76.
7. G. ALBINGER, Java Jandel Video Analysis Software (Jandel Scientific, Corte Madera, CA, 1988) p. 4.8.
8. W. J. FAN and R. A. VARIN, *Z. Metallkde.* **85** (1994) 522.
9. E. E. UNDERWOOD, "Quantitative Stereology" (Addison-Wesley, Reading, 1990).
10. W. D. CALLISTER, Jr, in "Materials Science and Engineering–An Introduction" (John Wiley, New York, 1991) p. 1.
11. C. T. LIU, J. O. STIEGLER and F. H. FROES, in "Metals Handbook", 10th Edn, Vol. 2 (American Society for Metals, Metals Park, OH, 1990) p. 913.
12. I. S. VIRK, M. B. WINNICKA and R. A. VARIN, *Scripta Metall. Mater.* **24** (1990) 2181.
13. H. LI, A. GHOSH, Y. H. HAN and R. C. BRADT, *J. Mater. Res.* **8** (1993) 1028.
14. J. BYSTRZYCKI and R. A. VARIN, *Scripta Metall.* **29** (1993) 605.

Received 2 August 1993
and accepted 16 May 1994